Chapter 1

THEORY OF VALENCE TRANSITIONS IN YTTERBIUM-BASED COMPOUNDS

V. Zlatić[1,3], and J. K. Freericks[2,3]
[1] *Institute of Physics, 10000 Zagreb, Croatia*
[2] *Department of Physics, Georgetown University, Washington, DC 20057, USA*
[3] *Isaac Newton Institute, Cambridge CB3 0EH, UK*

Abstract The anomalous behavior of $YbInCu_4$ and similar compounds is modeled by the exact solution of the spin one-half Falicov-Kimball model in infinite dimensions. The valence-fluctuating transition is related to a metal-insulator transition caused by the Falicov-Kimball interaction, and triggered by the change in the f-occupancy.

1. INTRODUCTION

The intermetallic compounds of the $YbInCu_4$ family exhibit an isostructural transition from high-temperature state with trivalent Yb ions in the $4f^{13}$ configuration to the low-temperature mixed-valent state with Yb ions fluctuating between $4f^{13}$ and $4f^{14}$ configurations [1]. The transition is particularly abrupt in high-quality stoichiometric $YbInCu_4$ samples [2] with a transition temperature equal to $T_v = 42$ K at ambient pressure; the susceptibility and the resistivity drop at T_v by more than one order of magnitude in cooling, while the volume expansion is small, $\Delta V/V \simeq 0.05$. The valence change inferred from $\Delta V/V$ by using the usual ionic radii of Yb^{3+} and Yb^{2+} is about $\Delta n_f \simeq 0.1$, which is consistent with the valence measurements by the L_{III}-edge absorption [1, 4]. The critical temperature depends strongly on external pressure, magnetic field, and alloying [5, 6]. A recent review of the experimental data is given in Ref. [7] and here we just recall the main points which motivate our choice of model.

The integer-valent phase ($T \geq T_v$) is characterized by a Curie-Weiss susceptibility [1, 6] with very small Curie-Weiss temperature $\Theta \ll T_v$. The Curie constant corresponds to the free moment of one magnetic f-hole in a $J = 7/2$ spin-orbit state with $\mu_{eff} = 4.53\mu_B$. The electrical resistance is large and has

a small positive slope; it remains almost unchanged in magnetic fields up to 30 T [5]. In some systems, like $Yb_{1-x}Y_xInCu_4$, the magnetoresistance is slightly negative, while in $YbInCu_4$ (or $YbIn_{1-x}Ag_xCu_4$ for $x = 0.15$) it is slightly positive [5]. The Hall constant is large and negative, indicating a small number of carriers [4, 8]. The thermoelectric power has a rather small slope which one finds in a semiconductor with a nearly symmetric density of states [9]. Recent data on the optical conductivity of $YbInCu_4$ [10] shows the absence of a Drude peak at high temperatures and a pronounced maximum of the optical spectral weight at about 1 eV. The high-temperature ESR data for Gd^{3+} embedded in $YbInCu_4$ resemble those found in integer-valence semi-metallic or insulator hosts [11]. Thus, the high-temperature phase indicates the presence of a well defined local moment but gives no signature of the Kondo effect. The overall behavior of the high-temperature phase is closer to that of a semi-metal or paramagnetic small-gap semiconductor than to a Kondo metal.

The mixed-valent phase ($T < T_v$) behaves like a Pauli paramagnet with moderately enhanced susceptibility and specific heat coefficient [6]. The electrical resistance and the Hall constant are one order of magnitude smaller than in the high-temperature phase [4, 8]. The thermoelectric power [9] has a very large slope typical of a valence fluctuator with large asymmetry in the density of states. The susceptibility, the resistivity and the Hall constant do not show any temperature dependence below T_v, which is also typical of valence fluctuators. The optical conductivity shows a major change with respect to the high-temperature shape. The peak around 1 eV is reduced, the Drude peak becomes fully developed, and an additional structure in the mid-infrared range appears quite suddenly below T_v [10]. A large density of states at the chemical potential μ is indicated by the ESR data as well [12]. Thus, the transition at T_v seems to be from a paramagnetic semimetal to a valence fluctuator.

In contrast to usual valence-fluctuators, which are quite insensitive to the magnetic field, the $YbInCu_4$ family of compounds also exhibit metamagnetic transitions when $T < T_v$. The Yb moment is fully restored at a critical field $H_c(T)$, with a Zeeman energy $\mu_B H_c$ comparable to the thermal energy $k_B T_v$. The metamagnetic transition defined by the magnetoresistance or the magnetization data [7] gives an H-T phase boundary $H_c(T) = H_c^0\sqrt{1-(T/T_v)^2}$. The zero-temperature field H_c^0 is related to T_v as $k_B T_v/\mu_B H_c^0 = 1.8$ [7].

To account for these features we need a model in which the non-magnetic, valence-fluctuating, metallic ground state can be destabilized by increasing temperature or magnetic field. Above the transition, we need a paramagnetic semiconductor with an average f-occupancy that is not changed much with respect to the ground state. The correct model for this system is a periodic Anderson model supplemented with a large Falicov-Kimball (FK) interaction term. The temperature or field induced transition suggests that one should place the narrow f-level just above the chemical potential μ. The hybridization keeps

the f-count finite below the transition, while large f-f correlations allow only the fluctuations between zero- and one-hole (magnetic) configurations. The low-temperature phase is close to the valence fluctuating fixed point and shows no Kondo effect. However, because of the Falicov-Kimball term, there is a critical f-occupation at which there is a transition into the high-temperature state with a large gap in the d- and f-excitation spectrum. The n_f is driven to criticality either by temperature or magnetic field. In the high-temperature phase the hybridization can be neglected because the f-level width is already large due to thermal fluctuations, and quantum fluctuations are irrelevant. Unfortunately, the above model would be difficult to solve in a controlled way, and here we consider a simplified model in which the hybridization is neglected at all temperatures. This leads to a spin-degenerate Falicov-Kimball model which explains the collapse of the non-magnetic metallic phase at T_v or H_c, and gives a good qualitative description of the high-temperature paramagnetic phase. However, the deficiency of the simplified model is that it yields a negligible f-count in the metallic phase and predicts a large change in the Yb valence at T_v or H_c. It is clear that we can not obtain the valence fluctuating ground state and maintain the average f-occupancy below the transition without hybridization-induced quantum fluctuations. In what follows, we describe the model, explain the method of solution, and present results for static and dynamic correlation functions.

2. CALCULATIONS

The Hamiltonian of the Falicov-Kimball model [13] consists of two types of electrons: conduction electrons (created or destroyed at site i by $d_{i\sigma}^{\dagger}$ or $d_{i\sigma}$) and localized electrons (created or destroyed at site i by $f_{i\sigma}^{\dagger}$ or $f_{i\sigma}$). The conduction electrons can hop between nearest-neighbor sites on the D-dimensional lattice, with a hopping matrix $-t_{ij} = -t^*/2\sqrt{D}$; we choose a scaling of the hopping matrix that yields a nontrivial limit in infinite-dimensions [14]. The f-electrons have a site energy E_f, and a chemical potential μ is employed to conserve the total number of electrons $n_{d\uparrow}+n_{d\downarrow}+n_{f\uparrow}+n_{f\downarrow} = n_{tot}$. The Coulomb repulsion U_{ff} between two f-electrons is infinite and there is a Coulomb interaction U between the d- and f-electrons that occupy the same lattice site. An external magnetic field h couples to localized electrons with a Landé g-factor. The resulting Hamiltonian is [15, 16]

$$\begin{aligned} H = &\sum_{ij,\sigma}(-t_{ij} - \mu\delta_{ij})d_{i\sigma}^{\dagger}d_{j\sigma} + \sum_{i,\sigma}(E_f - \mu)f_{i\sigma}^{\dagger}f_{i\sigma} \\ &+U\sum_{i,\sigma\sigma'} d_{i\sigma}^{\dagger}d_{i\sigma}f_{i\sigma'}^{\dagger}f_{i\sigma'} + U_{ff}\sum_{i,\sigma} f_{i\uparrow}^{\dagger}f_{i\uparrow}f_{i\downarrow}^{\dagger}f_{i\downarrow} \\ &-\mu_B h\sum_{i,\sigma}\sigma(2d_{i\sigma}^{\dagger}d_{i\sigma} + gf_{i\sigma}^{\dagger}f_{i\sigma}). \end{aligned} \tag{1.1}$$

The model can be solved in the infinite-dimensional limit by using the methods of Brandt-Mielsch [15]. We consider the hypercubic lattice with Gaussian density of states $\rho(\epsilon) = \exp[-\epsilon^2/t^{*2}]/\sqrt{\pi}t^*$, and take t^* as the unit of energy ($t^* = 1$). Our calculations are restricted to the homogeneous phase.

The local conduction-electron Green's function satisfies Dyson's equation

$$G^\sigma(z) = \int \frac{\rho(\epsilon)}{z + \mu - \Sigma^\sigma(z) - \epsilon} d\epsilon, \tag{1.2}$$

where z is a complex variable and Σ^σ is the local self energy which does not depend on momentum [14]. In infinite dimensions, Σ^σ is defined by a sum of skeleton diagrams, which depend on the local d-propagator G^σ but not on t_{ij}. The exact self-energy functional for the FK model is obtained by calculating the thermodynamic Green's function [17] of an atomic system coupled to an external time-dependent field $\lambda^\sigma(\tau)$

$$G^\sigma_{\rm atom}(\tau) = -\frac{1}{\mathcal{Z}} \mathrm{Tr}_{df} \left\langle T_\tau e^{-\beta H_{\rm atom}} d_\sigma(\tau') d^\dagger_\sigma(\tau) S(\lambda) \right\rangle, \tag{1.3}$$

where the S-matrix for the λ-field is

$$S(\lambda) = T_\tau e^{-\int_0^\beta d\tau \int_0^\beta d\tau' \lambda(\tau,\tau') d^\dagger_\sigma(\tau) d_\sigma(\tau')}, \tag{1.4}$$

and $H_{\rm atom}$ is obtained from the Hamiltonian (1.1) by removing the hopping and keeping just a single lattice site. The exact solution for $G^\sigma_n[\{\lambda_m\}]$ at Matsubara frequency $i\omega_n = i\pi T(2n+1)$ is given by,

$$G^\sigma_n = \frac{w_0}{[G^\sigma_{0n}]^{-1}} + \frac{w_1}{[G^\sigma_{0n}]^{-1} - U}, \tag{1.5}$$

where w_0 and w_1 are the f-occupation numbers ($w_1 = 1 - w_0$, $w_0 = \mathcal{Z}_0/\mathcal{Z}$) and [15]

$$\mathcal{Z}_0(\lambda,\mu) = 2e^{\beta\mu/2} \prod_n \frac{1}{(i\omega_n) G^\uparrow_{0n}} 2e^{\beta\mu/2} \prod_n \frac{1}{(i\omega_n) G^\downarrow_{0n}}, \tag{1.6}$$

with

$$\mathcal{Z}(\lambda,\mu) = \mathcal{Z}_0(\lambda,\mu) + 2e^{-\beta(E_f - \mu)} \mathcal{Z}_0(\lambda, \mu - U). \tag{1.7}$$

The bare Green's function satisfies

$$G^\sigma_{0n} = \frac{1}{i\omega_n + \mu - \lambda^\sigma_n}, \tag{1.8}$$

with λ_n the Fourier transform of the external time-dependent field.

The self-energy functional $\Sigma^\sigma_n[G^\sigma_n]$ can now be obtained [15] by using the Dyson equation for the atomic propagator,

$$\Sigma^\sigma_n = [G^\sigma_{0n}]^{-1} - [G^\sigma_n]^{-1}, \tag{1.9}$$

and eliminating $G^{\sigma}_{0n}[\{\lambda_m\}]$ from Eqs. (1.5) and (1.9). The mapping onto the lattice is achieved by adjusting G^{σ}_{0n} in such a way that $G^{\sigma}_{n}[\{\lambda_m\}]$ satisfies the lattice Dyson equation (1.2).

The numerical implementation of the above procedure is as follows: We start with an initial guess for the self energy Σ^{σ} and calculate the local propagator in (1.2). Using (1.9) we calculate the bare atomic propagator G^{σ}_{0n} and find $\mathcal{Z}_0$ and $\mathcal{Z}$. Next we obtain w_0, w_1 and find G^{σ}_{n} from (1.5). Using G^{σ}_{0n} and G^{σ}_{n}, we compute the atomic self energy and iterate to the fixed point.

The iterations on the imaginary axis give static properties, like n_f, the f-magnetization $m_f(h,t)$, and the static spin and charge susceptibilities. Having found the f-electron filling w_1 at each temperature, we iterate Eqs. (1.2) to (1.9) on the real axis and obtain the retarded dynamical properties, like the spectral function, the resistivity, the magnetoresistance, and the optical conductivity. At the fixed point, the spectral properties of the atom perturbed by λ-field coincide with the local spectral properties of the lattice.

3. RESULTS AND DISCUSSION

We studied the model for a total electron filling of 1.5 and for several values of E_f and U. The main results can be summarized in the following way.

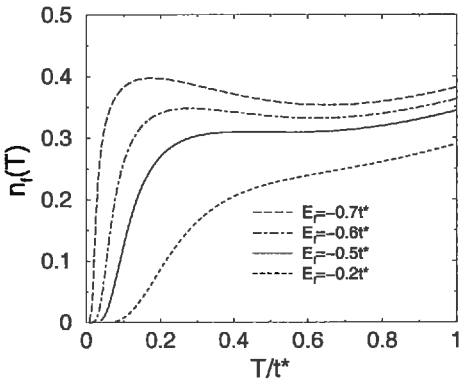

Figure 1.1 Number of the f-holes plotted versus T/t^* for $U/t^* = 4$. The E_f/t^* increases from top to bottom, and is given by -0.7, -0.6, -0.5, and -0.2, respectively.

The occupancy of the f-holes at high temperatures is large and there is a huge magnetic degeneracy. The f-holes are energetically unfavorable but are maintained because of their large magnetic entropy. In Fig.(1.1) we show n_f as a function of temperature, plotted for $U = 4t^*$, and E_f/t^* from -0.2 to -0.7. Below a certain temperature, which depends on U and E_f, there is a rapid transition to the low-temperature phase. The transition becomes sharper and is pushed to lower temperatures as E_f decreases at constant U. However, we

restrict ourselves to continuous crossovers here, since the region with first-order transitions leads to numerical instabilities.

The uniform f-spin susceptibility is obtained by calculating the spin-spin correlation function [15, 16] and is given by $\chi(T) = Cn_f(T)/T$, where $C = g_L^2\mu_B^2 J(J+1)/3k_B$ is the Curie constant. The $\chi(T)/C$ is shown in Fig. (1.2)

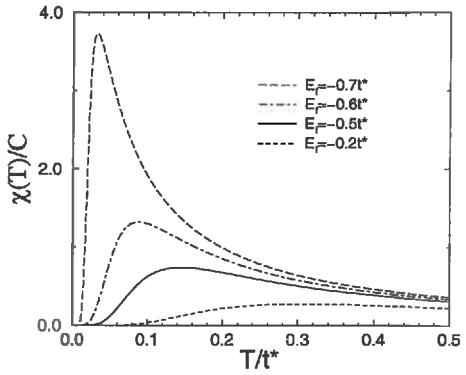

Figure 1.2 Uniform static magnetic susceptibility of the f-holes plotted versus T/t^* for $U/t^* = 4$. The values of E_f/t^* are the same as in Fig(1.1). The corresponding values of T_v/t^* are estimated from the maximum of $\chi(T)$, and are given by 0.03, 0.08, 0.15, 0.35, respectively. The T_v increases from top to bottom.

for $U/t^* = 4$ and for E_f as quoted in Fig.(1.1). The T_v is obtained from the maximum of the $\chi(T)/C$ and the values corresponding to various parameters used in this paper are quoted in the caption of Fig. (1.2). The high-temperature susceptibility follows an approximate Curie-Weiss law, but the Curie-Weiss parameters depend on the fitting interval.

The interacting density of states $\rho_d(\omega)$ for the conduction electrons is shown in Fig.(1.3) for $U/t^* = 4$ and $E_f/t^* = -0.5$, and for several temperatures. (The energy is measured with respect to μ.) The high-temperature DOS has a gap of the order of U, and the chemical potential is located within the gap. Below the transition n_f is small, the correlation effects are reduced, and $\rho_d(\omega)$ assumes a nearly non-interacting shape, with large $\rho_d(\mu)$ and halfwidth $W \simeq t^*$.

The transport properties of the high-T phase are dominated by the presence of the gap, which leads to a small dc conductivity with a weak temperature dependence. The transport properties of the paramagnetic phase are unrelated to the spin-disorder Kondo scattering (there is no spin-spin scattering in the FK model). Below the transition the conductivity increases and assumes large metallic values.

The intraband optical conductivity $\sigma(\omega)$ is plotted in Fig.(1.4) as a function of frequency, for several temperatures. Above T_v, we observe a reduced Drude peak around $\omega = 0$ and a pronounced high-frequency peak around $\omega \simeq U$. The

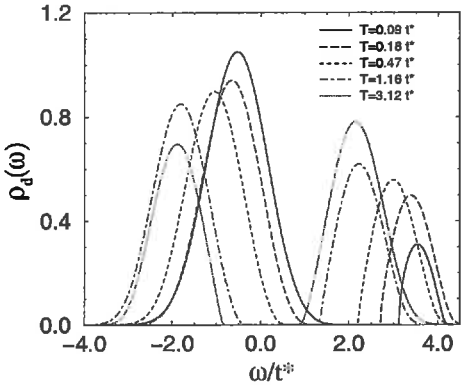

Figure 1.3 Interacting density of states plotted versus ω/t^* for $U/t^* = 4$, $E_f/t^* = -0.5$ ($T_v/t^* = 0.14$), and for various temperatures, as indicated in the figure.

shape of $\sigma(\omega)$ changes completely across T_v. Below T_v the Drude peak is fully developed and there is no high-energy (intraband) structure. However, if the renormalized f-level is close to μ, the interband d-f transition could lead to an additional mid-infrared peak. The ratio of the high-frequency peak in Fig(1.4) and the corresponding value of $T_v = 0.15t^*$, is $U/T_v = 26$. For the same value of U and $E_f = -0.7t^*$ ($T_v = 0.03t^*$) we obtain $U/T_v = 130$, while for $E_f = -0.75t^*$ ($T_v = 0.02t^*$) we find $U/T_v \simeq 200$ (not shown). If we

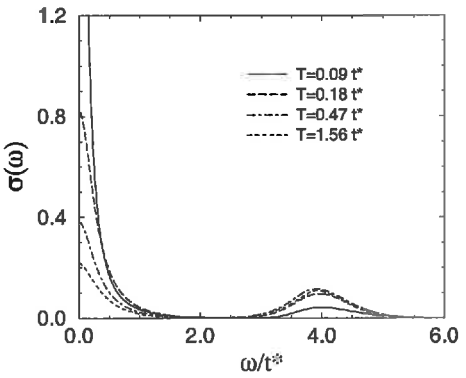

Figure 1.4 Optical conductivity plotted versus ω/t^* for various temperatures. The U, E_f, and T_v, are the same as in Fig.(1.3).

estimate the f-d correlation in $YbInCu_4$ from the 8000 cm^{-1} peak in the optical conductivity data [10], we obtain the experimental value $U \simeq 1$ eV. Together with $T_v = 42$ K [7] this gives the ratio $U/T_v \simeq 200$. If we take $U/t^* = 4$ and adjust E_f/t^* so as to bring the theoretical value of T_v in agreement with the the

thermodynamic and transport data on $YbInCu_4$, we get a high-frequency peak in $\sigma(\omega)$ at about 8000 cm^{-1}, 6000 cm^{-1}, and 1500 cm^{-1}, for $E_f = -0.75t^*$, $E_f = -0.7t^*$, and $E_f = -0.5t^*$, respectively.

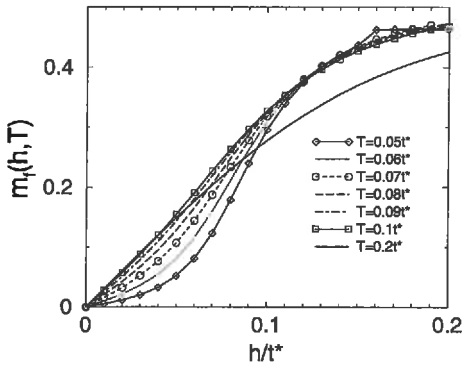

Figure 1.5 The f-electron magnetization m_f is plotted as a function of h/t^* for various temperatures. The U, E_f, and T_v, are the same as in Fig.(1.3).

The f-electron magnetization $m_f(h)$ is plotted in Fig.(1.5) versus reduced magnetic field h/t^*, for several temperatures. Above the characteristic temperature $T_v^* \simeq T_v/2$, the $m_f(h)$ curves exhibit typical local moment behavior. Below T_v^* we find a metamagnetic transition at a critical field H_c; the $m_f(h)$ is negligibly small below H_c and the local moment is fully restored above H_c. Taking the inflection point of the $m_f(h)$ curves, calculated for several values

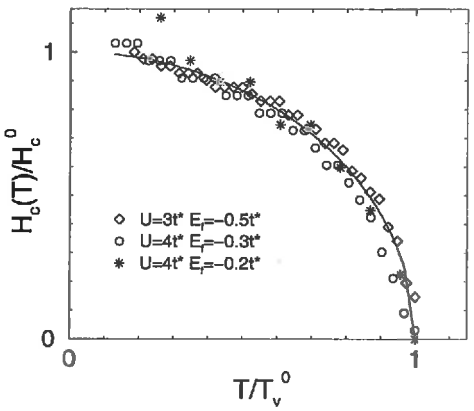

Figure 1.6 Normalized critical field is plotted as a function of reduced temperature T/T_v^* for several values of E_f/t^* and U/t^*. The full line represents $\sqrt{1-(T/T_v^*)^2}$ and $T_v^* = T_v/2$.

of U and E_f, as an estimate of $H_c(T)$ we obtain the phase boundary which is shown in Fig.(1.6), together with the expression $H_c(T)/H_c^0 = \sqrt{1-(T/T_v^*)^2}$.

Note, the T_v^* values in Fig.(1.6) differ by more than an order of magnitude, while the ratio $k_B T_v^*/\mu_B H_c^0$ is only weakly parameter dependent.

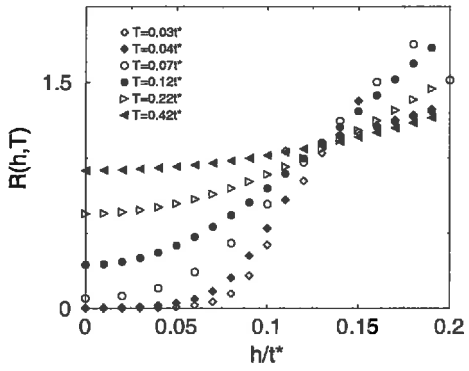

Figure 1.7 Field-dependent resistivity plotted versus h/t^*. The different symbols correspond to different temperatures, as indicated in the figure. The U and E_f are the same as in Fig.(1.3).

The metamagnetic transition is also seen in the field-dependent electrical resistance $R(h,T)$ which is plotted in Fig.(1.7) as a function of h/t^*, for several temperatures. A substantial change in the $R(h,T)$ across T_v^* or H_c is clearly seen.

4. SUMMARY

>From the preceding discussion it is clear that Falicov-Kimball model captures the main features of the experimental data for $YbInCu_4$ and similar compounds. The temperature- and field-induced anomalies are related to a metal-insulator transition, which is caused by large FK interaction and triggered by the temperature- or the field-induced change in the f-occupancy. At high temperatures, we find a large gap in $\rho_d(\omega)$; we expect a similar gap in the f-electron spectrum as well. At low temperatures, both gaps are closed, and the renormalized f-level renormalizes down to the chemical potential.

Our calculations describe doped Yb systems with broad transitions but appear to be less successful for those compounds which show a first-order transition. The numerical curves can be made sharper (by adjusting the parameters) but they only become discontinuous in a narrow parameter range. The main difficulty with the FK model is that it predicts a substantial change in the f-occupancy across the transition and associates the loss of moment with the loss of f-holes. But in the real materials the loss of moment seems to be due to the valence fluctuations, rather than to the reduction of n_f. The description of the valence fluctuating ground state would require the hybridization and is beyond the scope of this work. The actual situation pertaining to Yb ions in the mixed-valence state might be quite complicated, since one would have to consider an extremely

asymmetric limit of the Anderson model, in which the ground state is not Kondo-like, there is no Kondo resonance, and there is no single universal energy scale which is relevant at all temperatures [?].

We speculate that the periodic Anderson model with a large FK term will exhibit the same behavior as the FK model at high temperatures. Indeed, if the conduction band and the f-level are gapped, and the width of the f-level is large, then the effect of the hybridization can be accounted for by renormalizing the parameters of the FK model. On the other hand, if the low-temperature state of the full model is close to the valence-fluctuating fixed point with the conduction band and hybridized f-level close to the Fermi level, then the likely effect of the FK correlation is to renormalize the parameters of the Anderson model.

Acknowledgments

We acknowledge discussions with Z. Fisk, B. Lüthi, M. Miljak, M. Očko, and J. Sarrao. This research was supported by the National Science Foundation under grant DMR-9973225.

References

[1] I. Felner and I. Novik., Phys. Rev. B **33**, 617 (1986).

[2] J.L. Sarrao et al., Physics B, **223&224**, 366 (1996).

[3] J. M. Lawrence et al., Phys. Rev. B,**55**, 14 467 (1997).

[4] A. L. Cornelius et al., Phys. Rev. B,**56**, 7993 (1997).

[5] C. D. Immer et al., Phys. Rev. B,**56**, 71 (1997).

[6] J.L. Sarrao et al., Phys. Rev. B,**58**, 409 (1998)

[7] J.L. Sarrao, Physica B, **259&261**, 129 (1999)

[8] E. Figueroa et al., Solid State Commun. **106**, 347 (1998)

[9] M. Očko, J. Sarrao, Z. Fisk, unpublished.

[10] S. R. Garner et al., preprint (2000).

[11] T. S. Altshuler et al., Z. Phys. B**99**, 57 (1995).

[12] C. Rettori et al., Phys. Rev. B,**55**, 1016 (1997).

[13] L. M. Falicov and J. C. Kimball, Phys. Rev. Lett. **22**, 997 (1969).

[14] W. Metzner and D. Vollhardt, Phys. Rev. Lett. **62**, 324 (1989).

[15] U. Brandt and C. Mielsch, Z.Phys. B **75**, 365 (1989); U. Brandt and M. P. Urbanek, ibid. **89**, 297 (1992).

[16] J. Freericks and V. Zlatić, Phys. Rev. B **58**, 322 (1998).

[17] L.P. Kadanoff and G. Baym, *Quantum Statistical Physics* (W. A. Benjamin, Menlo Park, CA), 1962

[18] H. B. Krishnamurti et al., Phys. Rev. B **21**, 1044 (1980).

Chapter 1

THEORY OF VALENCE TRANSITIONS IN YTTERBIUM BASED COMPOUNDS

V. Zlatić[1,2], and J. K. Freericks[3]
[1] *Institute of Physics, 10000 Zagreb, Croatia*
[2] *Isaac Newton Institute, Cambridge CB3 0EH, UK*
[3] *Department of Physics, Georgetown University, Washington, DC 20057, USA*

Abstract The anomalous behavior of $YbInCu_4$ and similar compounds is modeled by the exact solution of the spin one-half Falicov-Kimball model in infinite dimensions. The valence-fluctuating transition is related to a metal-insulator transition caused by the Falicov-Kimball interaction, and triggered by the change in the f-occupancy.

1. INTRODUCTION

The intermetallic compounds of the $YbInCu_4$ family exhibit an isostructural transition from high-temperature state with trivalent Yb ions in the $4f^{13}$ configuration to the low-temperature mixed-valent state with Yb ions fluctuating between $4f^{13}$ and $4f^{14}$ configurations [1]. The transition is particularly abrupt in high-quality stoichiometric $YbInCu_4$ samples [2] with a transition temperature equal to $T_v = 42$ K at ambient pressure; the susceptibility and the resistivity drop at T_v by more than one order of magnitude in cooling, while the volume expansion [3] and the valence change [1, 4] are small ($\Delta V/V \simeq 0.05$ and $\Delta n_f \simeq 0.1$, respectively). Using the usual ionic radii of trivalent and divalent Yb, the relative change of the lattice parameter is found to be consistent with the valence change seen in the L_{III}-edge absorption. The critical temperature depends strongly on external pressure, magnetic field, and alloying (chemical pressure) [5, 6]. A recent review of the experimental data is given in Ref. [7] and here we just recall the main points which motivate our theoretical model.

The integer-valent phase ($T \geq T_v$) is characterized by a Curie-Weiss susceptibility [1, 6] with very small Curie-Weiss temperature $\Theta \ll T_v$. The Curie constant corresponds to the free moment of one magnetic f-hole in a $J = 7/2$

spin-orbit state with $\mu_{eff} = 4.53\mu_B$. The electrical resistance is large and has a small positive slope; it remains almost unchanged in magnetic fields up to 30 T [5]. In some systems, like $Yb_{1-x}Y_xInCu_4$, the magnetoresistance is slightly negative, while in $YbInCu_4$ (or $YbIn_{1-x}Ag_xCu_4$ for $x = 0.15$) it is slightly positive [5]. The Hall constant is large and negative, indicating a small number of carriers [4, 8]. The thermoelectric power has a rather small slope which one would find in a semiconductor with a nearly symmetric density of states [9]. Recent data on the optical conductivity of $YbInCu_4$ [10] shows the absence of a Drude peak at high temperatures and a pronounced maximum of the optical spectral weight at about 1 eV. The high-temperature ESR data for Gd^{3+} embedded in $YbInCu_4$ resemble those found in integer-valence semi-metallic or insulator hosts [11]. The striking feature of the high-temperature phase is the presence of a well defined local moment but the absence of any signature of the Kondo effect. The overall behavior of the high-temperature phase is similar to that of a semi-metal or paramagnetic small-gap semiconductor.

The mixed-valent phase ($T < T_v$) behaves like a Pauli paramagnet with moderately enhanced susceptibility and a specific heat coefficient [6] $\gamma \simeq 50mJ/molK^2$. The electrical resistance and the Hall constant are one order of magnitude smaller than in the high-temperature phase [4, 8]. The thermoelectric power [9] has a very large slope which is typical of a valence fluctuator with large asymmetry in the density of states. The susceptibility, the resistivity and the Hall constant do not show any temperature dependence below T_v, which is also typical of valence fluctuators. The optical conductivity is Drude like but there is also an additional structure in the mid-infrared range, which appears quite suddenly below T_v [10]. A large density of states at the chemical potential μ is indicated not just by the transport data but also by the ESR data [12].

In contrast to usual valence-fluctuators, which are quite insensitive to the magnetic field, the $YbInCu_4$ family of compounds also exhibit metamagnetic transitions when $T < T_v$. The Yb moment is fully restored at a critical field $H_c(T)$, with a Zeeman energy $\mu_B H_c$ comparable to the thermal energy $k_B T_v$. The metamagnetic transition defined by the magnetoresistance or the magnetization data [7] gives an H-T phase boundary $H_c(T) = H_c^0\sqrt{1-(T/T_v^0)^2}$. The zero-field temperature T_v^0 and the zero-temperature field H_c^0 are found to be related as $k_B T_v^0/\mu_B H_c^0 = 1.8$.

To account for these features we need a model in which the non-magnetic, valence-fluctuating, metallic ground state can be destabilized by increasing temperature or magnetic field. Above the transition, we need a paramagnetic semiconductor with an average f-occupancy that is not changed much with respect to the ground state. The correct model for this system is a periodic Anderson model supplemented with a large Falicov-Kimball (FK) interaction term. The temperature or field induced transition suggests that one should place the narrow f-level just above the μ, so that the metallic ground state can be

destabilized by either thermal fluctuations or a magnetic field. The hybridization keeps the f-count finite below the transition, while large f-f correlations allow only the fluctuations between zero- and one-hole (magnetic) configurations. The low-temperature phase is close to the valence fluctuating fixed point and shows no Kondo effect. However, because of the FK term, there is a critical f-occupation at which there is a transition into the high-temperature state which has a gap in the excitation spectrum and has all states shifted with respect to μ. In the high-temperature phase the hybridization can be neglected because the f-level width is already large due to thermal fluctuations, and quantum fluctuations are irrelevant. Unfortunately, the above model would be difficult to solve in a controlled way, and here we consider a simplified model in which the hybridization is neglected at all temperatures. This leads to spin-degenerate FK model which explains the collapse of the non-magnetic metallic phase at T_v or H_c, and gives a good qualitative description of the high-temperature paramagnetic phase. However, the deficiency of the simplified model is that it yields a negligible f-count in the metallic phase and predicts a large change in the Yb valence at T_v or H_c. It is clear that we can not obtain the valence fluctuating ground state and maintain the average f-occupancy below the transition without hybridization-induced quantum fluctuations. In what follows, we describe the model, explain the method of solution, and present results for static and dynamic correlation functions.

2. CALCULATIONS

The Hamiltonian of the FK model [13] consists of two types of electrons: conduction electrons (created or destroyed at site i by $d^\dagger_{i\sigma}$ or $d_{i\sigma}$) and localized electrons (created or destroyed at site i by $f^\dagger_{i\sigma}$ or $f_{i\sigma}$). The conduction electrons can hop between nearest-neighbor sites, with a hopping matrix $-t_{ij} = -t^*/2\sqrt{D}$, where we have chosen to examine hypercubic lattices in D-dimensions, and we choose a scaling of the hopping matrix that yields a nontrivial limit in infinite-dimensions [14]. The bare density of states $\rho(\epsilon)$ on a hypercubic lattice is a Gaussian

$$\rho(\epsilon) = \frac{1}{\sqrt{\pi}t^*} \exp[-\epsilon^2/t^{*2}], \tag{1.1}$$

and we take t^* as the unit of energy ($t^* = 1$). The f-electrons have a site energy E_f, and a chemical potential μ is employed to conserve the total number of electrons $n_{d\uparrow} + n_{d\downarrow} + n_{f\uparrow} + n_{f\downarrow} = n_{tot}$. The Coulomb repulsion U_{ff} between two f-electrons is infinite and there is a Coulomb interaction U between the d- and f-electrons that occupy the same lattice site. An external magnetic field h couples to localized electrons with a Landé g-factor. The resulting Hamiltonian

is [15, 16]

$$H = \sum_{ij,\sigma}(-t_{ij} - \mu\delta_{ij})d^\dagger_{i\sigma}d_{j\sigma} + \sum_{i,\sigma}(E_f - \mu)f^\dagger_{i\sigma}f_{i\sigma} + U\sum_{i,\sigma\sigma'} d^\dagger_{i\sigma}d_{i\sigma}f^\dagger_{i\sigma'}f_{i\sigma'} + U_{ff}\sum_{i,\sigma} f^\dagger_{i\uparrow}f_{i\uparrow}f^\dagger_{i\downarrow}f_{i\downarrow} - \mu_B h\sum_{i,\sigma}\sigma(2d^\dagger_{i\sigma}d_{i\sigma} + gf^\dagger_{i\sigma}f_{i\sigma}). \quad (1.2)$$

The model can be solved in the infinite-dimensional limit by using the methods of Brandt-Mielsch [15]. Our calculations are restricted to the homogeneous phase.

The local conduction-electron Green's function satisfies Dyson's equation

$$G^\sigma(z) = \int \frac{\rho(\epsilon)}{z + \mu - \Sigma^\sigma(z) - \epsilon}d\epsilon, \quad (1.3)$$

where z is a complex variable and Σ^σ is the local self energy which does not depend on momentum [14]. In infinite dimensions, Σ^σ is defined by a sum of skeleton diagrams, which depend on the local d-propagator G^σ but not on t_{ij}. The exact self-energy functional for the FK model is obtained by calculating the thermodynamic Green's function [17] of an atomic system coupled to an external time-dependent field $\lambda^\sigma(\tau)$

$$G^\sigma_{\rm atom}(\tau) = -\frac{1}{\mathcal{Z}}{\rm Tr}_{df}\left\langle T_\tau e^{-\beta H_{atom}}d_\sigma(\tau')d^\dagger_\sigma(\tau)S(\lambda)\right\rangle, \quad (1.4)$$

where the S-matrix for the λ-field is

$$S(\lambda) = T_\tau e^{-\int_0^\beta d\tau\int_0^\beta d\tau'\lambda(\tau,\tau')d^\dagger_\sigma(\tau)d_\sigma(\tau')}, \quad (1.5)$$

and H_{atom} is obtained from the Hamiltonian (1.2) by removing the hopping and keeping just a single lattice site. The exact solution for $G^\sigma_n(\lambda_n)$ at Matsubara frequency $\omega_n = \pi T(2n+1)$ is given by,

$$G^\sigma_n = \frac{w_0}{[G^\sigma_{0n}]^{-1}} + \frac{w_1}{[G^\sigma_{0n}]^{-1} - U}, \quad (1.6)$$

where w_0 and w_1 are the f-occupation numbers ($w_1 = 1 - w_0$, $w_0 = \mathcal{Z}_0/\mathcal{Z}$) and [15]

$$\mathcal{Z}_0(\lambda,\mu) = 2e^{\beta\mu/2}\prod_n \frac{1}{(i\omega_n)G^\uparrow_{0n}}2e^{\beta\mu/2}\prod_n \frac{1}{(i\omega_n)G^\downarrow_{0n}}, \quad (1.7)$$

with

$$\mathcal{Z}(\lambda,\mu) = \mathcal{Z}_0(\lambda,\mu) + 2e^{-\beta(E_f-\mu)}\mathcal{Z}_0(\lambda,\mu-U). \quad (1.8)$$

The bare Green's function satisfies

$$G^{\sigma}_{0n} = \frac{1}{i\omega_n + \mu - \lambda^{\sigma}_n}, \tag{1.9}$$

with λ_n the Fourier transform of the external time-dependent field.

The self energy functional $\Sigma^{\sigma}_n[G^{\sigma}_n]$ can now be obtained [15] by using the atomic Dyson equation

$$\Sigma^{\sigma}_n = [G^{\sigma}_{0n}]^{-1} - [G^{\sigma}_n]^{-1}, \tag{1.10}$$

and eliminating $G^{\sigma}_{0n}[\{\lambda_m\}]$ from Eqs. (1.6) and (1.10). The mapping onto the lattice is achieved by adjusting G^{σ}_{0n} in such a way that $G^{\sigma}_n[\{\lambda_m\}]$ satisfies the lattice Dyson equation (1.3).

The numerical implementation of the above procedure is as follows: We start with an initial guess for the self energy Σ^{σ} and calculate the local propagator in (1.3). Using (1.10) we calculate the bare atomic propagator G^{σ}_{0n} and find $\mathcal{Z}_0$ and $\mathcal{Z}$. Next we obtain w_0, w_1 and find the atomic Green's function G^{σ}_n from (1.6). Using G^{σ}_{0n} and G^{σ}_n, we compute the atomic self energy and iterate to the fixed point.

The iterations on the imaginary axis give static properties, like n_f, the f-magnetization $m_f(h,t)$, and the static spin and charge susceptibilities. Having found the f-electron filling w_1 at each temperature, we iterate Eqs. (1.3) to (1.10) on the real axis and obtain the retarded properties, like the spectral function, the resistivity, the magnetoresistance, and the optical conductivity. At the fixed point, the spectral properties of the atom preturbed by λ-field coincide with the local spectral properties of the lattice.

3. RESULTS AND DISCUSSION

We discuss the FK model for a total electron filling of 1.5, $U/t^* = 4$, and E_f/t^* from -0.2 to -0.7, with the ensuing values of T_v/t^* between 0.02 and 0.07. The main results can be summarized as follows:

Above T_v, the occupancy of the f-holes is large and the system has a huge magnetic degeneracy. The f-holes are energetically unfavorable but are maintained because of their large magnetic entropy. In Fig.(1.1) we show n_f as a function of temperature, plotted for several values of E_f. Below a certain value of $n_f(T)$ there is a rapid transition to the low-temperature phase. The transition becomes sharper and is pushed to lower temperatures as E_f decreases. However, we restrict ourselves to continuous crossovers here, since the region with first-order transitions leads to numerical instabilities.

The uniform f-spin susceptibility is obtained by calculating the spin-spin correlation function [15, 16] and is given by $\chi(T) = Cn_f(T)/T$, where $C = g^2_L\mu^2_B J(J+1)/3k_B$ is the Curie constant and $n(T)$ is a slowly varying function

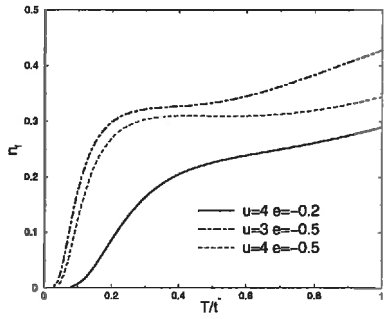

Figure 1.1 Number of the f-holes plotted versus T/t^*. Different curves correspond to $E_f/t^* = -0.5, -0.6$ and -0.7 (the E_f increases from top to bottom) with $T_v/t^* = 0.07$, 0.04, and 0.02 respectively.

for $T > T_v$. $\chi(T)/C$ is shown in Fig. (1.2) for the same parameters. The high-temperature data follow an approximate Curie-Weiss law. However, the Curie-Weiss parameters depend on the fitting interval, and Θ is unrelated to T_v. Below T_v, the f-susceptibility is negligibly small; the total susceptibility is due to conduction electrons and is Pauli like.

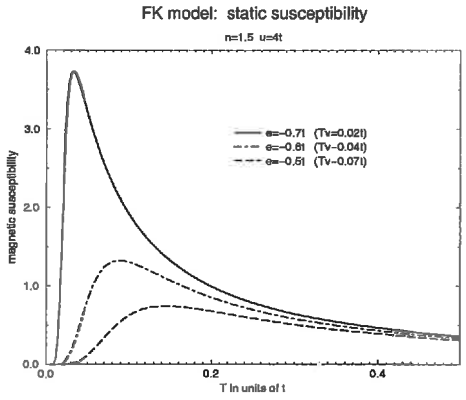

Figure 1.2 Uniform static magnetic susceptibility of the f-holes plotted versus T/t^*. Different curves correspond to $E_f/t^* = -0.5, -0.6$ and -0.7 (the E_f increases from top to bottom) with $T_v/t^* = 0.07$, 0.04, and 0.02 respectively.

The interacting density of states $\rho_d(\omega)$ for the conduction electrons is shown in Fig.(1.3). For U=4, $\rho_d(\omega)$ has a large gap at high temperatures, with the chemical potential located within the gap. Below the transition n_f is small, the correlation effects are reduced, and $\rho_d(\omega)$ assumes a nearly non-interacting shape, with μ in the high-DOS region.

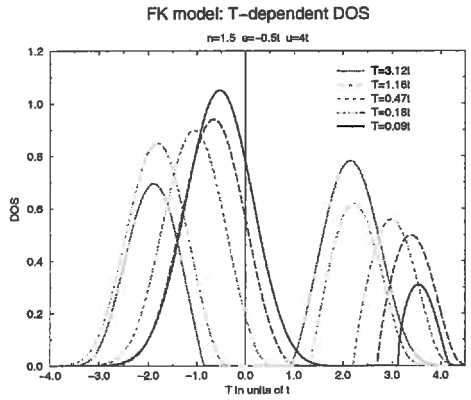

Figure 1.3 Interacting density of states plotted versus ω/t^* for various temperatures, as indicated in the figure.

The transport properties of the high-T phase are dominated by the presence of the gap, which leads to a small temperature-independent dc conductivity. The transport properties of the paramagnetic phase are unrelated to the spin-disorder Kondo scattering, as there is no spin-spin scattering in the model. Below the transition the conductivity increases and assumes large metallic values.

The intra-band optical conductivity $\sigma(\omega)$ is plotted in Fig.(1.4) as a function of frequency, for several temperatures. Above the transition, $\sigma(\omega)$ has a high-energy peak around $\omega \simeq U$ and a greatly reduced Drude peak. At low temperatures, the Drude peak is fully developed and there is no intra-band high-energy structure. However, we expect the renormalized f-level to now be close to μ and the inter-band d-f transition could lead to the appearance of an additional mid-infrared peak.

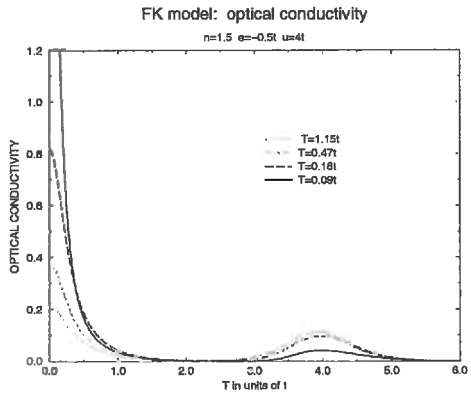

Figure 1.4 Optical conductivity plotted versus ω/t^* for various temperatures. as indicated in the figure.

Calculations in finite magnetic field show that the local moment is restored for H larger than a critical field H_c that is strongly parameter dependent. The field induced f-electron magnetization $m(H)$ is plotted in Fig.(1.5) as a function of H, and shows a typical metamagnetic transition. There is a qualitative difference in the $m_f(H)$ curves for $T < T_v^0$ and $T > T_v^0$.

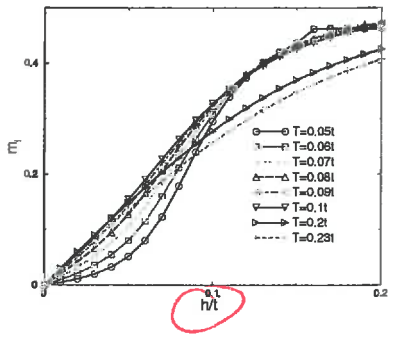

Figure 1.5 The f-electron magnetization m_f is plotted as a function of the magnetic field for different temperatures, as indicated in the figure. Here $E_f/t^* = -0.5$ and $T_v^0/t^* = 0.07$.

The metamagnetic transition is also seen in the field-dependent electrical resistance which is shown in Fig.(1.6). The effect of the magnetic field on the resistance is much more pronounced for $T < T_v^0$ than for $T > T_v^0$.

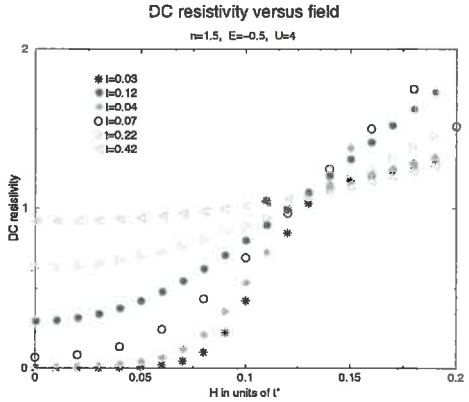

Figure 1.6 Field-dependent resistivity plotted versus H for various temperatures. The different simbols correspond to different temperatures, as indicated in the figure.

Taking the inflection point of the $m(H)$ curves as an estimate of $H_c(T)$ we find that the phase boundary can be fit by the expression, $H_c(T) = H_c^0\sqrt{1-(T/T_v^0)^2}$, as shown in Fig.(1.7) for several values of U and E_f. The ratio $k_b T_v^0/\mu_B H_c^0$ is found to be between 1.5 and 2.0. A similar result follows from Fig.(1.6).

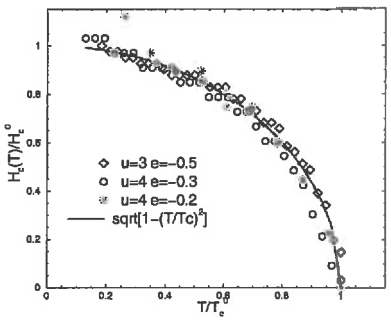

Figure 1.7 Critical field normalized as a function of temperature. H_c^0 is the zero-temperature critical field, and T_c^0 is the zero-field critical temperature. The different curves correspond to $E/t^* = -0.5, -0.6$ and -0.7 and their respective T_c^0 values differ by more than an order of magnitude.

4. SUMMARY

From the preceding discussion it is clear that Falicov-Kimball model captures the main features of the experimental data for $YbInCu_4$ and similar compounds. The temperature and field induced anomalies are related to a metal-insulator transition, which is caused by the FK interaction and triggered by the change in the f-occupancy. The behavior of correlation functions across T_v indicate that the renormalized f-level E_f^* shifts in cooling from high to low energies. Actually, we expect the high-temperature gap which we find for large U in $\rho_d(\omega)$ to appear in the f-electron spectrum as well.

Our calculations describe doped Yb systems with broad transitions but appear to be less successful for those compounds which show a first-order transition. The numerical curves can be made sharper (by adjusting the parameters) but they only become discontinuous in a narrow parameter range. The main difficulty with the FK model is that it predicts a substantial change in the f-occupancy across the transition and associates the loss of moment with the loss of f-holes. But in the real materials the loss of moment seems to be due to the valence fluctuations, rather than to the reduction of n_f. The description of the valence fluctuating ground state would require additional terms in the Hamiltonian and is beyond the scope of this work. The actual situation pertaining to Yb ions in the mixed-valence state might be quite complicated, since one would have to consider an extremely asymmetric limit of the Anderson model ($E_f^* \simeq \mu$ and $U_{ff} = \infty$). In this limit, the ground state is not Kondo-like, there is no Kondo resonance, and there is no single universal energy scale which is relevant at all temperatures [18].

It is tempting to speculate that the periodic Anderson model with a large FK term will exhibit the same behavior as the FK model at high temperatures. Indeed, if the conduction band and the f-level are gapped, and the width of the f-level is large, the effect of the hybridization can be accounted for by renormalizing the parameters of the standard FK model. On the other hand, if the low-temperature state of the full model is close to the valence-fluctuating fixed point with the conduction band and hybridized f-level close to the Fermi level, then the effect of the FK correlation is to renormalize the parameters of the usual Anderson model.

Acknowledgments

We acknowledge useful disussions with I. Aviani, Z. Fisk, B. Lüthi, M. Miljak, M. Očko, and J. Sarrao. This research was supported by the National Science Foundation under grant DMR-9973225.

References

[1] I. Felner and I. Novik., Phys. Rev. B **33**, 617 (1986); I. Felner, et al., Phys. Rev. B **35**, 6956 (1987).

[2] J.L. Sarrao et al., Physics B, **223&224**, 366 (1996)

[3] J. M. Lawrence et al., Phys. Rev. B,**55**, 14 467 (1997).

[4] A. L. Cornelius et al., Phys. Rev. B,**56**, 7993 (1997).

[5] C. D. Immer et al., Phys. Rev. B,**56**, 71 (1997).

[6] J.L. Sarrao et al., Phys. Rev. B,**58**, 409 (1998)

[7] J.L. Sarrao, Physica B, **259&261**, 129 (1999)

[8] E. Figueroa et all, Solid State Commun. **106**, 347 (1998)

[9] M. Očko, J. Sarrao, Z. Fisk, unpublished

[10] S. R. Garner et al., preprint (2000)

[11] T. S. Altshuler et al., Z. Phys. B**99**, 57 (1995).

[12] C. Rettori et al., Phys. Rev. B,**55**, 1016 (1997).

[13] L. M. Falicov and J. C. Kimball, Phys. Rev. Lett. **22**, 997 (1969).

[14] W. Metzner and D. Vollhardt, Phys. Rev. Lett. **62**, 324 (1989).

[15] U. Brandt and M. P. Urbanek, Z.Phys. B **89**, 297 (1992).

[16] J. Freericks and V. Zlatić, Phys. Rev. B **58**, 322 (1998).

[17] L.P. Kadanoff and G. Baym, *Quantum Statistical Physics* (W. A. Benjamin, Menlo Park, CA), 1962

[18] H.B. Krishnamurti et al., Phys. Rev. B, **21**, 1044 (1980).

Recent Newton Institute Preprints

NI00001-SMM **KZ Markov**
Justification of an effective field method in elasto-statics of heterogeneous solids

NI00002-SCE **YY Lobanov and VD Rushai**
Studying the evolution of open quantum systems via conditional Wiener integrals

NI00003-SCE **J-G Wang and G-S Tian**
Spin and charged gaps in strongly correlated electron systems with negative or positive couplings

NI00004-SCE **FV Kusmartsev**
Conducting electron strings in oxides

NI00005-ERN **SG Dani**
On ergodic Z^d actions on Lie groups by automorphisms

NI00006-SMM **V Nesi and G Alessandrini**
Univalence of σ-harmonic mappings and applications

NI00007-SCE **X Dai, T Xiang, T-K Ng et al**
Probing superconducting phase fluctuations from the current noise spectrum of pseudogaped metal-superconductor tunnel junctions

NI00008-ERN **B Hasselblatt**
Hyperbolic dynamical systems

NI00009-SCE **J Lou, S Quin, T-K Ng et al**
Topological effects at short antiferromagnetic Heisenberg chains

NI00010-SCE **V Zlatić and J Freericks**
Theory of valence transitions in Ytterbium-based compounds

NI00011-ERN **A Iozzi and D Witte**
Cartan-decomposition subgroups of SU(2,n)

NI00012-ERN **D Witte and L Lifschitz**
On automorophisms of arithmetic subgroups of unipotent groups in positive characteristic

NI00013-ERN **D Witte**
Homogeneous Lorentz manifold with simple isometry group

NI00014-SGT **R Uribe-Vargos**
Global theorems on vertics and flattenings of closed curves

NI00015-SGT **EA Bartolo, P Cassou-Nogués, I Luengo et al**
Monodromy conjecture for some surface singularities

NI00016-SGT **IG Scherbak**
Boundary singularities and non-crystallographic Coxeter groups

NI00017-SGT **K Houston**
On the classification and topology of complex map-germs of corank one and $\mathcal{A}_e$-codimension one

NI00018-SGT **PJ Topalov and VS Matveev**
Geodesic equivalence via integrability

NI00019-GTF **S Friedlander**
On vortex tube stretching and instabilities in an inviscid fluid

NI00020-SGT **VD Sedykh**
Some invariants of admissible homotopies of space curves

NI00021-SGT **IA Bogaevsky**
Singularities of linear waves in plane and space

Information about Newton Institute Preprints is also available at
`http://www.newton.cam.ac.uk/preprints.html`